Slope Failure Surface Using Finite Element Method

Ahn, Tae-Bong*

요 지

사면안정해석을 수행하기 위하여 많이 사용하는 한계평형방법은 일정한 가정을 하여 안전율을 평형에 필요한 응력과 흙의 전단강도의 비로 정의하여 대상사면의 안전율을 구한다. 유한요소법을 이용한 사면안정해석방법은 응력상태를 유한요소법으로 구한 후 원호나 대수나선형등의 일정한 모양의 사면파괴선을 가정하여 반복적으로 최소안전율을 구한다. 본 연구에서는 유한요소법을 이용한 사면안정해석방법을 개발하여 사면의 가장 취약한 부분을 따라 파괴선이 발생하도록 하였다. 이것은 요소내의 국부안전율과 파괴각을 고려하여 사면파괴선을 자동적으로 구할 수 있도록 함으로써 가능한데 이 방법은 임의의 파괴선을 가정할 필요가 없으며 절편에 작용하는 힘에 대하여 가정을 할 필요가 없고 임의의 모양의 파괴선을 구할 수 있는 장점이 있다. 본 연구에서는 개발된 해석방법을 검증하기 위하여 가상의 사면, 자연사면, 그리고 댐사면에 적용하여 실무에서 많이 사용하는 한계평형방법 프로그램인 STABL5M과 SLOPE/W과 비교 평가하였다.

Abstract

In limit equilibrium methods(LEM), all methods employ the same definition of the safety factor as a ratio of the shear strength of the soil to the shear stress required for equilibrium, employing certain assumptions with regard to equilibrium. In addition, in the conventional finite element method of analysis, the minimum safety factor is obtained assuming certain slip surfaces after the state of stress are found. Although the stress states are obtained from the finite element method (FEM), the slope stability analysis follows the conventional method that assumes a potential slip surface. In this study, a slope stability analysis based on FEM is developed to locate the slip surface by tracking the weakest points in the slope based on the local safety factor considering the magnitude and direction of the shear stresses. It has also been applied to be compared with the slip surfaces predicted by LEM. A computer program has been developed to draw contour lines of the local safety factors automatically. This method is illustrated through a simple hypothetical slope, a natural soil slope, and a dam slope. The developed method matches very well with the conventional LEM methods, with slightly lower global safety factors.

Keywords : Slope stability, FEM, Local safety factor, Slip surface, Element equation

* Member, Senior Researcher, Korea Institute of Construction Technology

1. Introduction

Slope stability analysis methods can be classified into two general methods; the limit equilibrium method and the finite element method. The limit equilibrium method is utilized without a prior knowledge of the location and geometry of the slip surface. A potential slip surface, either circular or log-spiral geometry or others, is then assumed and the minimum safety factor is found through an iterative search. In the LEM, the number of available equations is smaller than the number of the unknown. Therefore, all limit equilibrium methods of slope stability analysis need to employ assumptions to render the problem determinate.

In the LEM, all methods employ the same definition of the safety factor, i.e.) the ratio between the shear strength of the soil and the shear stress required for equilibrium with certain assumptions. An implicit assumption in the limit equilibrium methods of slopes stability analysis is that the stress-strain behavior is ductile. Also, the main assumption in the LEM is a constant safety factor along the slip surface. This limitation results from the fact that the methods provide no information regarding the magnitudes of the strains within the slope, nor any indication about how they may vary along the slip surface(Duncan, 1996). The safety factor obtained by LEM varies with the assumptions employed in the analysis. In the FEM, however, the safety factors calculated are not constant within the entire slope(Wright et al., 1973). Tavenas et al. (1980) have noted that the safety factor varies along the slip surface. This is closer to real situation because the slip surface would follow the weakest points in the slope.

In this study, a FEM slope stability analysis method is developed to find the optimal slip surface by tracking the weakest points within the slope and the results are applied to the soil slope to be compared with the slip surfaces obtained from LEM methods.

2. Slope Stability Analysis

2.1 Limit Equilibrium Method

In the Geotechnical Engineering, a sufficient safety factor against failure must be provided. In the slope stability analysis, the most general definition of the safety factor is defined as:

$$F = \frac{shear\ strength\ of\ soil}{shear\ stress\ required\ for\ equilibrium} \tag{1}$$

Lowe(1967) indicated that defining the safety factor as a factor of shear strength is logical, because the shear strength is the quantity that involves the greatest degree of uncertainty. However, the main disadvantage of LEM is that the deformation analysis is not possible and the strain distribution along the slip surface is not available. In general, since the peak strength is not mobilized simultaneously along the entire length of the slip surface after the shearing resistance drops off after reaching the peak, a progressive failure may occur and the shearing resistance at

some points may be smaller than the peak strength. A fully reliable approach in such cases is to use the residual strength rather than the peak strength in the analysis (Duncan, 1996). The stress-strain characteristic is specially important for strain softening soils such as overconsolidated clays and dense sands.

2.2 Finite Element Method

In general, the slope stability analysis is performed assuming a slip surface, and the slope is considered safe if the resulting safety factor is greater than one. However, slopes frequently became unstable due to bulging, stress concentrations, and cracks although the overall safety factor may be over one. Therefore, the deformation analysis has been regarded important in predicting the detailed slope deformation behavior. The general characteristics of the finite element method of the slope stability analysis are as follows:

(1) It can calculate the stress, strain, and pore water pressure.

(2) It can analyze the consolidation, swelling, and dissipation of excess pore water pressure under certain conditions during or post-construction.

(3) It is useful to investigate the cracks and local failures within the slope.

Donald and Giam (1988) used the nodal displacements obtained from the finite element analysis to determine the factor of safety with respect to the stability of slopes. Giam and Donald (1988) presented an approach that used an automatic search scheme to locate the critical slip surface. Huang and Yamasaki (1993) analyzed the slope stability using local minimum safety factor, and employed the Drucker-Prager model, which is a elato-plastic stress-strain model using the Automatic Dynamic Incremental Nonlinear Analysis (ADINA) finite element program.

3. Development of Finite Element Method Program

The FEM method is flexible enough to model many complex conditions with a high degree of realism, e.g.) the nonlinear stress-strain behavior, non-homogeneous conditions, and changes in geometry during the construction of a slope (Duncan, 1996).

The program developed in this study utilizes the local safety factor in slope, and predicts the slip surface by connecting the lines of shearing angle in each element. The program utilizes quadrilateral elements.

The followings are the main characteristics of the developed FEM program.

(1) The program calculates the safety factors in all elements, and predicts the failure surface tracking the weakest points considering the shear failure angle in each element.

(2) The slip surface can be successfully utilized in soil and weathered rock slopes.

(3) The shape of the slip surface does not need to be assumed.

(4) The results of the analysis are incorporated with the postprocessor.

Finite element procedures of stress analysis are explained in the following sections more detailedly.

3.1 Initial Stress in Soil

In a soil mass, initial geostatic stresses exist due to the overburden. The initial stress state significantly affects the initial modulus necessary for the nonlinear or plastic analysis for subsequent loading. For an undisturbed soil mass, the initial stresses correspond to the in-situ stresses at rest. At that state, the horizontal stress is related to the vertical stress by the coefficient of lateral earth pressure at rest. For any point below a sloping ground, the stress may be expressed as (Figure 1)

$$\sigma_v = \gamma z \cos \beta \tag{2a}$$

and

$$\sigma_h = K\gamma z \cos \beta \tag{2b}$$

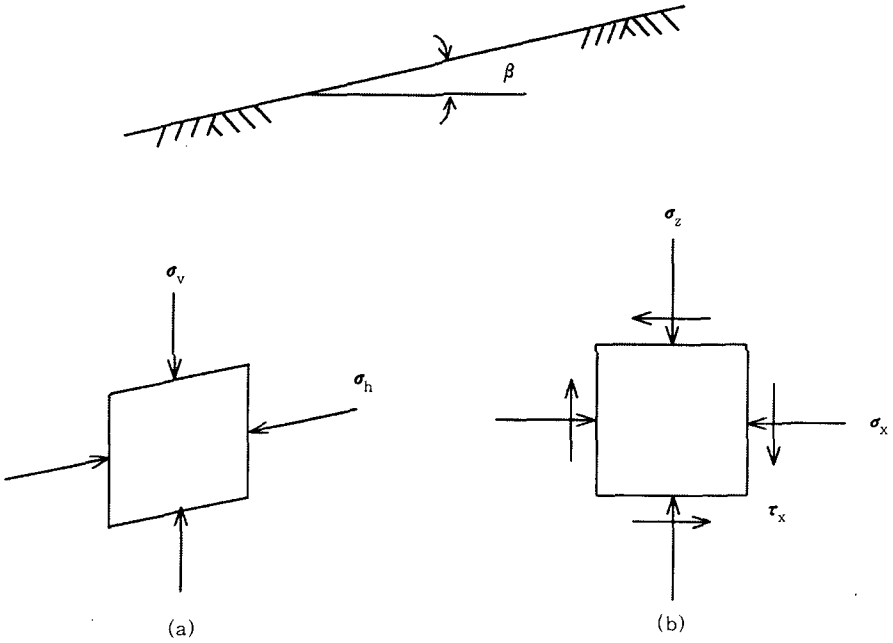

Fig. 1. The stress state of slope

where σ_v, σ_h are the vertical and horizontal stresses, γ is the unit weight of the soil, z is the depth to the point, K is the conjugate stress ratio, and β is the slope angle. Horizontal stress, σ_x which is proportional to the vertical stress acting at the same point with a consideration of stress components on the x-z plane, the vertical stresses, σ_z, and the shear stress, τ_{xz} are obtained as follows (Chowdhury, 1978).

$$\begin{aligned} \sigma_z &= \gamma z(1 + K \sin^2 \beta) \\ \sigma_x &= K\gamma z \cos^2 \beta \\ \tau_{xz} &= K\gamma z \sin \beta \cos \beta \end{aligned} \tag{3}$$

where $K=\frac{K_o+r_u(1-K_o)}{\cos^2\beta-K_o\sin^2\beta}$; $r_u=\frac{u}{\gamma z}$ = pore water pressure ratio, u = pore water pressure, and K_o = coefficient of earth pressure at rest.

From equation (3), principal stresses and corresponding rotation angles can be calculated as

$$\sigma_{1,3}=\gamma z\left\{\frac{1+K}{2}\pm\frac{1}{2}\sqrt{K^2+2K\ \sin^2\beta-2K\ \cos^2\beta+1}\right\} \tag{4}$$

When $\beta=0$, it is easily seen that $\sigma_1=\gamma z$ and $\sigma_3=K\gamma z$ as expected. The principal stresses are inclined at angle θ to the x-axis given by

$$\tan 2\theta=\frac{2K\ \sin\beta\ \cos\beta}{K\ \cos^2\beta-1-K\ \sin^2\beta} \tag{5}$$

It is noted that the configuration of the slope is assumed to be a two-dimensional case, and therefore the intermediate principal stress is not included.

3.2 Finite Element Formulation

The stress-strain analysis considers the effect of the seepage on the stress analysis as follows. First, the initial stresses of the soil mass are computed as explained in section 3.1. Next, the fluid nodal head of the seepage flow is computed. For each element, the centroidal pore pressure is identified. The seepage force and subsequently the resultant body force are then computed. The change in body force due to seepage is calculated by subtracting of the present value from the previously stored value. The incremental nodal forces are then assembled into a global vector and a finite element analysis is performed. The resulting stresses and deformations due to the incremental loading are then added into the existing values. The procedure used here for the finite element analysis is explained briefly below:

(1) The finite element method procedure used in this work at the element level is expressed as

$$[k]\{q\}=\{Q_e\}+\{Q_s\}=\{Q\} \tag{6}$$

where $[k]$ is the stiffness matrix, $\{q\}$ is the vector of nodal displacements, $\{Q_e\}$ is the vector of the external forces, $\{Q_e\}$ is the vector of the seepage forces, and $\{Q\}$ is the vector of external and seepage forces.

(2) The initial stress in the soil mass due to the body force is computed by solving the following equations:

$$[k]^o\{q\}=\{Q_e\}^o \tag{7}$$

and

$$\{\sigma\}^o=[F]^o\{q\}^o \tag{8}$$

where $[k]^{\circ}$ is the initial stiffness matrix, $\{q\}$ is the initial deformation vector, $\{Q_e\}^{\circ}$ is the initial body force vector, $\{\sigma\}^{\circ}$ is the initial stress vector, and $[F]^{\circ}$ is the initial stress-displacement transformation matrix. The superscript "o" indicates the initial condition.

(3) At each time step, the seepage state is solved and the seepage forces are calculated on the basis of the computed nodal heads from the seepage analysis at each element center. The seepage force is then combined with the gravity force to form a nodal force vector. The following equations are solved in order to obtain the changes in displacements, $\{\Delta q\}^i$, due to the changes in seepage forces, $\{\Delta Q_s\}^i$,

$$[k]^i\{\Delta q\}^i = \{Q\}^i - \{Q\}^{i-1} = \{\Delta Q_s\}^i \tag{9}$$

where $[k]^i$, is the updated stiffness matrix and $\{\Delta q\}^i$ is the incremental displacement vector. The stiffness matrix, $[k]^i$, is the updated to allow the nonlinear material behavior.

(4) The seepage force is explained as follows and described in Figure 2.

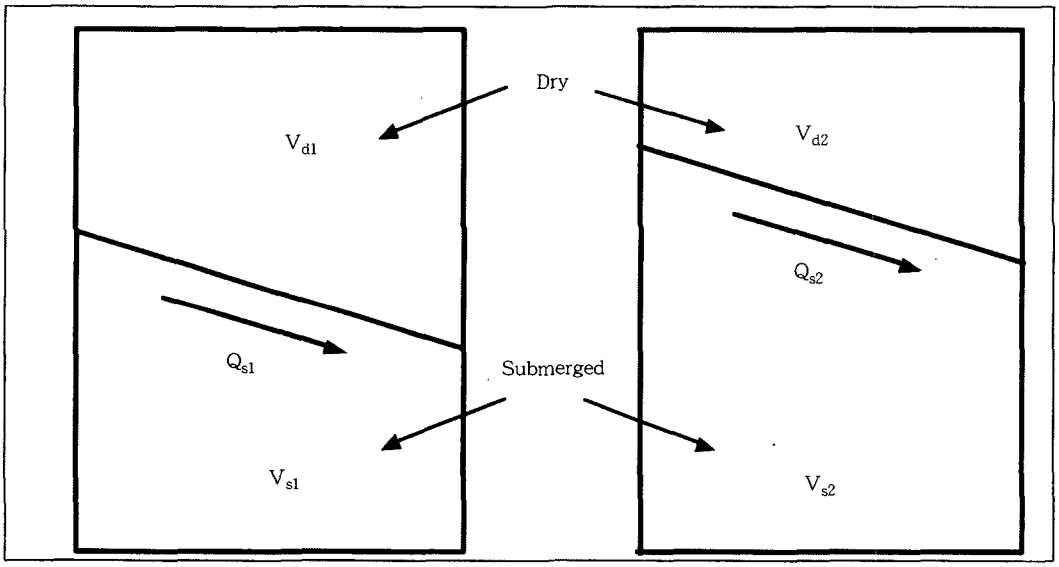

Fig. 2. Schematic diagram of soil element at two time levels

Consider a soil at two different time steps. The change in seepage force, $\{\Delta Q_s\}^i$, between the two time step is given by

$$\{\Delta Q_s\} = \{Q_s\}_2 - \{Q_s\}_1 \tag{10a}$$

where

$$\{Q_s\}_2 = \begin{Bmatrix} \gamma_d V_{d2} + (\gamma_s - \gamma_w)V_{s2} + Q_{sz2} \\ Q_{sx2} \end{Bmatrix} \tag{10b}$$

$$\{Q_s\}_1 = \begin{Bmatrix} \gamma_d V_{d1} + (\gamma_s - \gamma_w)V_{s1} + Q_{sz1} \\ Q_{sx1} \end{Bmatrix} \tag{10c}$$

where γ_d is the dry unit weight, γ_s is the saturated unit weight, V_d is the volume of the dry soil, V_s is the volume of the saturated soil, and Q_{sx}, and Q_{sz} are the components of the seepage force vector $\{Q_s\}$. $\{Q_s\}$ is obtained from

$$\{Q_s\} = \iiint_V [B]^T \{p\} dV \tag{10d}$$

where {p} is the fluid pressure vector, and [B] is the strain-displacement transformation matrix.

(5) From the incremental displacement vector, the incremental stress vector is computed and added to the existing stress vector:

$$\{q\}^i = \{q\}^{i-1} + \{\Delta q\}^i \tag{11a}$$

$$\{\sigma\}^i = \{\sigma\}^{i-1} + \{\Delta\sigma\}^i \tag{11b}$$

where $\{\Delta q\}^i$ are the incremental displacements, and $\{\Delta\sigma\}^i$ and $\{\sigma\}^i$ are the incremental and total stress vectors, respectively, and $\{\sigma\}^{i-1}$ is the total stress vector of the previous step. Finally, coordinates of all nodal points are updated according to the incremental nodal displacements, and the stiffness matrix is also updated. The procedure is repeated at each time step. The major concern is the use of appropriate constitutive model. In elasto-plastic analysis, it is necessary to deal with stress and strain increments instead of total stress and strain levels that represent the nonlinearlity of stress strain behavior. In this study, tangent modulus method is used. During each iteration, total stress stiffness matrix is updated according to the stress-strain relation. The stress-strain relationship assumes a linear elastic model in the elastic range and a perfectly plastic range in the post-yield region.

4. Safety Factor of Slope Stability

The computer code includes the computation of safety factors based on the hyperbolic nonlinear elastic and the Drucker-Prager elasto-plastic soil characterizations. These safety factors are calculated at the element level. In the former case, the local safety factor of each element is described as:

$$(f.s)_e = \frac{\bar{c} + \bar{\sigma}_n \tan\phi}{\tau} \tag{12}$$

where $\bar{c}$ is cohesive strength, $\bar{\sigma}_n$ is normal stress, ϕ is internal friction angle, τ is induced shear stress, and the overbar denotes effective quantities. The local safety factor of each element is obtained on the basis of the computed stresses as described in Eq. (12). The stress state of the each element can be described with the Mohr Circle in Figure 3. Point "P" on the Mohr Circle in Figure 3 represents the state of stresses whose normal makes an angle of $\theta/2$ in a clockwise direction from the major principal stress direction, σ_1. From the diagram, the local safety factor of Eq. (12) can be found. The orientation and the value of $f.s_{\min}$ can be obtained through following steps:

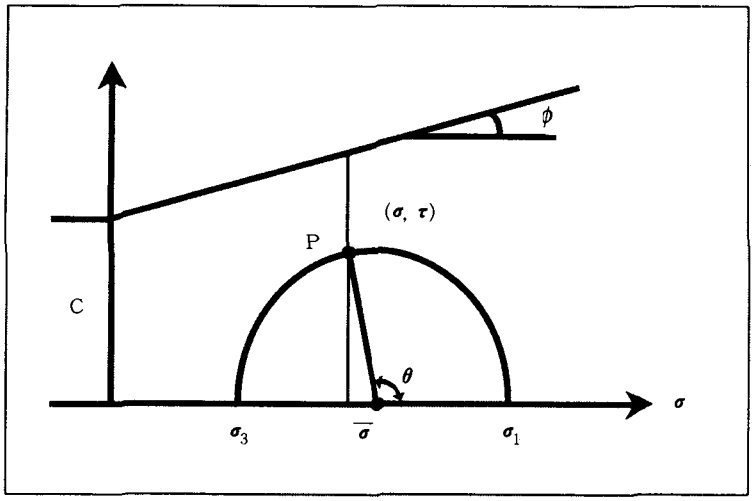

Fig. 3. Stress state of the each element on Mohr circle

$$\tau = r\sin\theta$$
$$\sigma = \bar{\sigma} + r\cos\theta \tag{13a}$$

where, $$r = \frac{\sigma_1 - \sigma_3}{2},\quad \bar{\sigma} = \frac{\sigma_1 + \sigma_3}{2} \tag{13b}$$

$$f.s = \frac{c + \sigma\tan\phi}{r\sin\theta} = \frac{c + (\bar{\sigma} + r\cos\theta)\tan\phi}{r\sin\theta} \tag{13c}$$

The minimum safety factor can be obtained by differentiating the safety factor with respect to the angle, , i.e.,

$$\frac{\partial f.s}{\partial\theta} = \frac{-B\sin\theta r\ \sin\theta - (A + B\cos\theta)r\cos\theta}{r^2\sin^2\theta}$$
$$= \frac{-Br(\sin^2\theta + \cos^2\theta) - Ar\ \cos\theta}{r^2\sin^2\theta} = \frac{B + A\cos\theta}{r\sin^2\theta} = 0 \tag{13d}$$

the solution occurs when

$$\cos\theta = -\frac{B}{A}$$

This leads to $$\theta_{\min} = \cos^{-1}\frac{B}{A},\quad A = c + \bar{\sigma}\tan\phi,\quad B = r\tan\phi \tag{13e}$$

Two values of $\theta_{\min}$ are possible because the Mohr circle has positive and negative values of the shear stress. These are the two potential sliding planes on which the safety factor is minimum. The overall safety factor is the weighted average of the minimum local safety factors along the entire

slip surface:

$$F.S = \frac{\sum_{i}^{n} (f.s)_e a_e}{L} \tag{14}$$

where a_e is the length of the slip surface intersecting the element, L is total length of the slip surface, and n is the number of elements on the slip surface.

In this analysis, a sequential procedure is adopted. First, the minimum local safety factor is obtained using Eq. (13). Secondly, the orientation of the slip surface is found by tracking the minimum local safety factor using the shear failure angle. At this stage, using the iterative procedure, the optimum slip surface is connected along the minimum local safety factors. While the slip surface is connected, the overall safety factor is calculated as described in Eq. (14). By an iterative procedure, the slip surface showing the minimum overall safety factor is determined.

5. Examples

Three slope examples have been examined in this study; a simple slope, an embankment slope, and a natural soil slope. The results are compared with the results of STABL5M, which is a limit equilibrium method.

5.1 Simple Hypothetical Slope

This slope is made for analysis and is shown in Figure 3. The soil strength parameters are $c' = 4.9\text{kN/m}^2$, $\phi' = 30°$, and $\gamma = 19.6\text{kN/m}^3$.

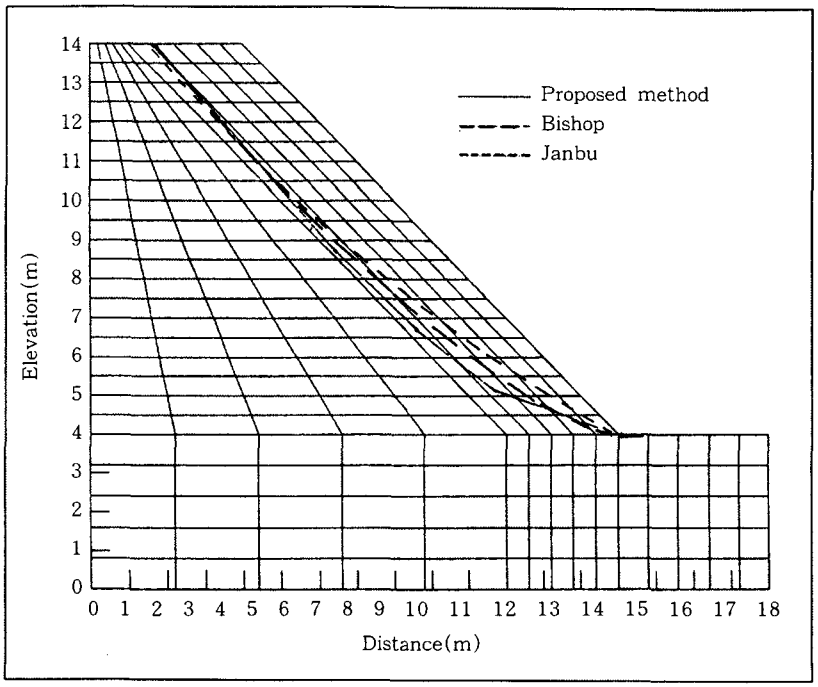

Fig. 4 The slip surfaces of hypothetical slopes

In this analysis, results of STABL5M are 0.968 and 0.978 in safety factor for Janbu's method and Bishop's method respectively. In the finite element analysis, 275 elements and 328 nodes are used for the analysis. The four node quadrilateral element is used, and the element number is varied. The employed material properties are shown in Table 1. The slip surfaces were found from STABL5M and developed methods are compared one unother in Figure 4.

The slip surface of developed procedure is slightly lower than the results of STABL5M. The overall safety factor from the proposed method is 0.95 lower than the safety factor from other methods. In this example, the ground water level is neglected, so the input data for γ_{dry} and γ_{sat} of program are considered as 19.6kN/m^3 for simple case.

Table 1. The material properties of hypothetical slope

	Dry Soil	Wet Soil
Elastic Moduls(E, MPa)	51	68.6
Poisson Ratio(v)	0.485	0.380
Internal Friction Angle(ϕ, deg)	30	30
Cohesion(c, kN/m^2)	4.9	4.9
Unit Weight(γ, kN/m^3)	19.6	19.6

5.2 Embankment Slope

The hypothetical dam has soil properties similar to the Springfield Dam studied by Huang and Yamasaki (1993). The result is compared with those of the Huang and Yamasaki's method and of the STABL5M. The safety factor from this study is 1.01 while those obtained from STABLE5M and Huang and Yamasaki's method are 1.12 and 1.05 respectively. In Figure 5, the total number of elements and nodes employed are 100 and 121, respectively. The material properties of the employed soils are as shown in Table 2.

The slip surface determined from the proposed method is between those obtained from the STABL5M(i.e, Bishop's method) and the Huang and Yamasaki's method.

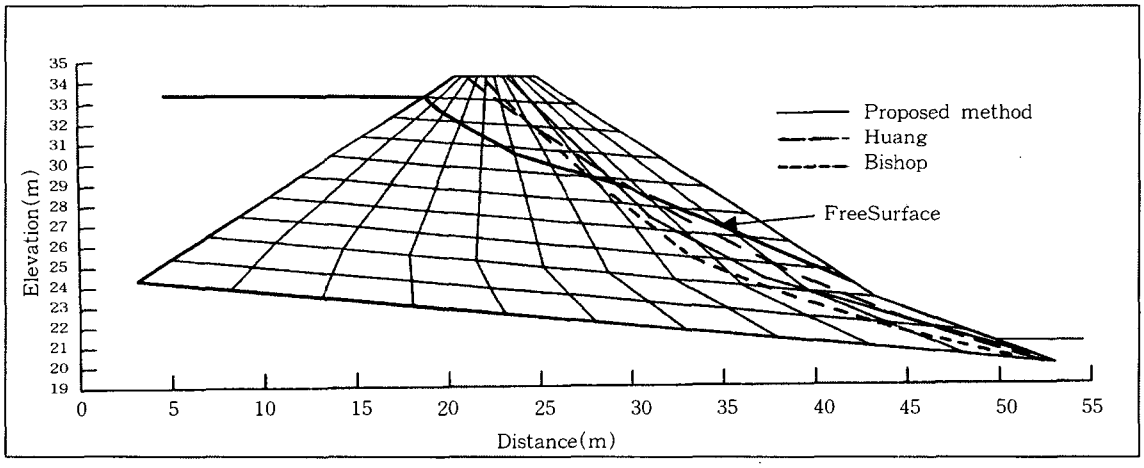

Fig. 5. The slip surfaces of Springfield dam

Table 2. The material properties of embankment slope

	Dry Soil	Wet Soil
Elastic Moduls(E, MPa)	20	28
Poisson Ratio(v)	0.33	0.290
Internal Friction Angle(ϕ, deg)	25	25
Cohesion(c, kN/m^2)	9.6	9.6
Unit Weight(γ, kN/m^3)	19.6	21

5.3 Natural Soil Slope

The proposed method has been applied to an existing natural soil slope in Danyang. The slope failure was first initiated after a heavy rainfall in 1972. Since the slope is located next to the Nam-Han river, central part of South Korea, additional landslides may block the flow of river water causing a flood to Danyang city(Figure. 6). The site investigation involved 15 bore holes, inclinometer measurements, shear strength tests of the soil, and rock strength tests. The determination of soil properties was difficult because the soil slope is made of colluvial soils. The soil properties are shown in Table 3, and the finite element grid of the slope is shown in Figure 7, which consists of 80 elements and 99 nodes. Slope stability analysis was performed along three sections, and the slip surfaces were compared with the results from the Bishop's method. Figure 7 shows the results of analysis on section A-A. The predicted slip surface is located at a deeper depth than that of the Bishop's method. Since the slip surface was determined by connecting the minimum local safety factor using θ_{min}, the global safety factor is generally lower than that of the limit equilibrium method of which failure surface is predetermined. As a previous research, Huang

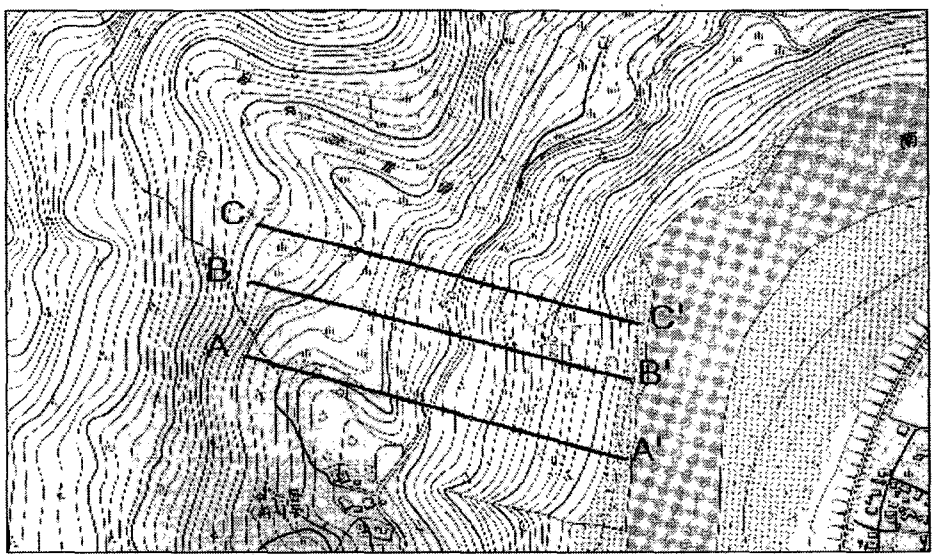

Fig. 6 The geological map of Danyang slope

and Yamasaki(1993) found the slip surface from the vector line. In this analysis, however, optimal interconnection of the failure angle of each element is employed. This is why the slip surface is different from those of the previous analysis results. Figures 8 and 9 show the slip surfaces of Section B-B and Section C-C. Same soil parameters with that of A-A section were used for the analysis, where the geometries are somewhat different. The slip surfaces were obtained by the proposed method, program SLOPE/W, and STABL5M. As expected, the overall safety factors of the proposed method show somewhat lower value than other methods.

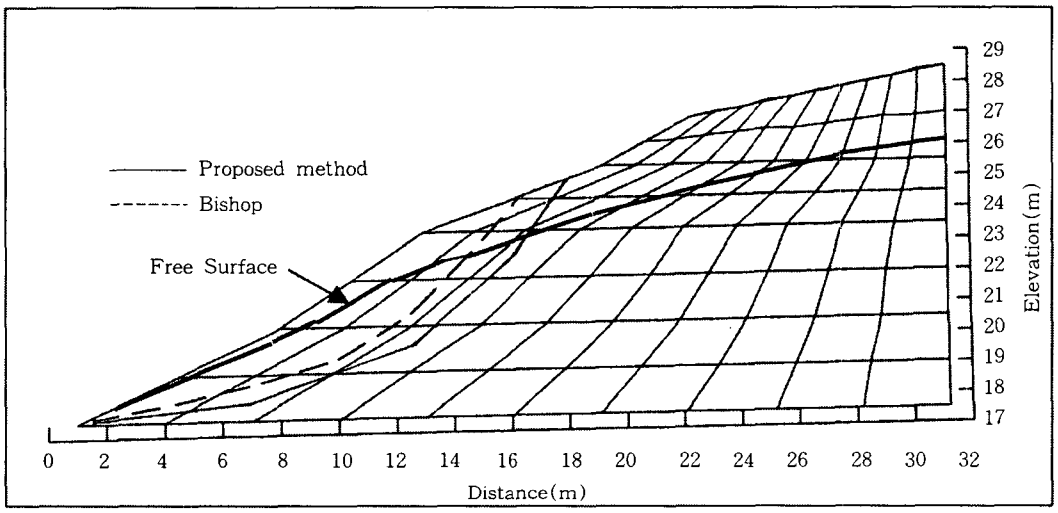

Fig. 7 Comparison of slip surfaces between proposed method and Bishop's method (A-A section)

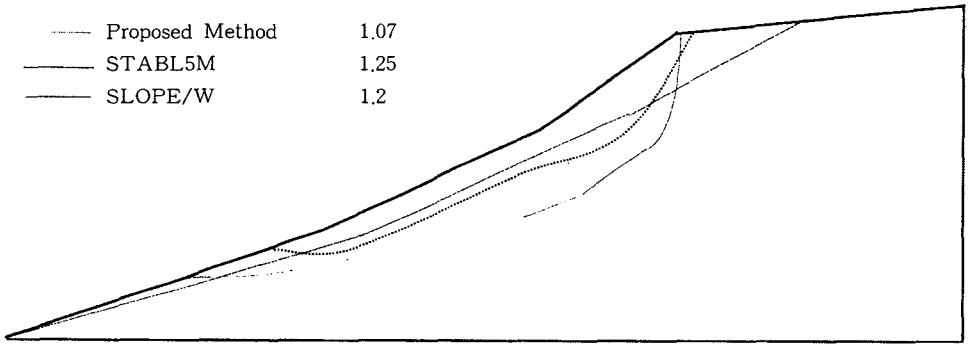

Fig. 8 Comparison of slip surfaces between proposed FEM method and LEM (B-B section)

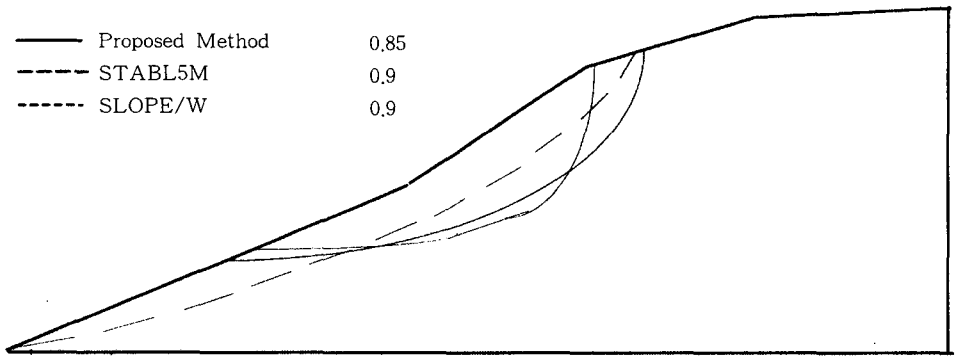

Fig. 9 Comparison of slip surfaces between proposed FEM method and LEM(C-C section)

Table 3. The material properties of natural soil slope

	Dry Soil	Wet Soil
Elastic Moduls(E, MPa)	56.8	70.6
Poisson Ratio(ν)	0.45	0.38
Internal Friction Angle(ϕ, deg)	25	25
Cohesion(c, kN/m^2)	14.4	14.4
Unit Weight(γ, kN/m^3)	19.6	21

6. Conclusions

Examples included in this paper illustrate the use of the local safety factors and failure inclination angles of each finite element for the slope stability analysis. The proposed method can be considered as an alternative approach to existing slope stability analysis methods. It shows slightly lower safety factor with the location of slip surface being somewhat different. The advantage of the proposed method is that the slip surface does not need to be assumed, rather it is calculated. Also, the employed concerning side force and its location that often should be employed in limit method do not need to be considered, as they are included in the present method.

References

1. Chowdhury, R. N. (1978), "Slope Analysis", *El Servier*, pp. 221-234.
2. Desai, C. S. and Siriwardane, H. J. (1984), "Constitutive Laws for Engineering Materials with Emphasis on Geologic Materials", *Prentice-Hall Inc*, pp. 83-91, 244-246.
3. Donald, I. B. and Giam, S. K. (1988), "Application of The Nodal Displacement Method to Slope Stability Analysis", *Proc. 5th Australia-New Zealand Conf. on Geomech.* Sydney, Australia, pp. 456-460.
4. Duncan, J. M. (1996), "State of The Art: Limit Equilibrium and Finite Element Analysis of Slope",

Journal of Geotechnical Engineering, Vol. 122, No 7, pp. 577-596.

5. Giam, S. K. and Donald, I. B. (1988), "Determination of Critical Slip Surfaces for Slopes via Stress-Strain Calculations", *Proc. 5th Australia-New Zealand Conf. on Geomech*, Sydney, Australia, pp. 461-464.
6. Huang, S. L. and Yamasaki, K. (1993), "Slope Failure Analysis Using Local Minimum Factor of Safety Approach", *Journal of Geotechnical Engineering*, ASCE, Vol. 119, No. 12, pp. 1974-1987.
7. Huang, S. L., Speck, R. C. and Yamasaki, K (1989), "Direct Determination of Failure Surface in Earth Slopes", *Proc. 30th U.S. Symp. on Rock Mech., International Society for Rock Mechanics/U.S. National Committee for Rock Mechanics*, pp. 817-824.
8. Li, G. C. and Desai, C. S.0 (1983), "Stress and Seepage Analysis of Earth Dams," *Journal of Geotechnical Engineering. ASCE*, Vol. 112, No 6, pp. 946-960.
9. Lowe, J. and Karafiath, L. (1959), "Stability of Earth Dams upon Drawdown", Panamerican *Conference on Soil Mechanics and Foundation Engineering*, Mexico
10. Lowe, J. (1967).. "Stability Analysis of Embankments", *Journal of Soil Mech and Found. Div., ASCE*, Vol. 93 No 4, pp. 1-33.
11. Segerlind, L. J. (1976), "Applied Finite Element Analysis", *John Wiley*, New York.
12. Tavenas, F., Trak, B. and Leroueil, S (1980), "Remarks on the Validity of Stability Analyses", *Canadian Geotechnical Journal*, 17(1), pp. 61-73.
13. Wright, S. G., Kulhawy, F. H., and Duncan, J. M. (1973), "Accuracy of Equilibrium Slope Stability Analysis", *Journal of the Soil Mechanics and Foundations Division*, ASCE Vol. 99, No. SM10, pp 783-791.

(received Apr., 2. 1999)